Journal of Metals, Materials and Minerals, 35(1), e1919, 2025

Enhancing acetone gas sensor performance with cobalt oxide doping in $LaFeO_3$ prepared by co-precipitation

Andhy SETIAWAN[1], Farah Aprisza SHEELMAREVAA[1], Muhamad Taufik ULHAKIM[2], Dani Gustaman SYARIF[3], and Endi SUHENDI[1*]

[1] *Physics Study Program, Faculty of Mathematics and Natural Sciences Education, Universitas Pendidikan Indonesia, Jl. Dr. Setiabudi No. 229, Isola, Sukasari, Bandung, West Java, 40154, Indonesia*

[2] *Department of Mechanical Engineering, Faculty of Engineering, Universitas Buana Perjuangan Karawang, Jl. HS Ronggo Waluyo, Puseurjaya, Telukjambe Timur, Karawang, West Java, 41361, Indonesia*

[3] *National Research and Innovation Agency (BRIN), Jl. Tamansari No. 71 Lebak Siliwangi, Coblong, Bandung, West Java, 40132, Indonesia*

***Corresponding author e-mail**: endis@upi.edu

Received date:
15 September 2024
Revised date:
11 December 2024
Accepted date:
24 February 2025

Keywords:
Dopant effect;
Acetone gas sensor;
Cobalt oxide;
$LaFeO_3$;
Co-precipitation

Abstract

Semiconductor-based gas sensors frequently encounter difficulties in attaining optimal performance due to challenges such as temporal stability and low sensitivity, stemming from their insulating properties at room temperature. To address these limitations, this study proposes a novel approach by preparing cobalt-doped $LaFeO_3$ ($LaFeO_3$-Co) using the co-precipitation method, with doping concentrations of 2.5 mol% and 5.0 mol%. The acetone gas sensors were fabricated into thick films via the screen-printing technique, and their performance was thoroughly characterized. X-ray diffraction (XRD) analysis confirmed a cubic crystal structure, and the addition of 2.5 mol% cobalt was found to reduce the particle size of $LaFeO_3$, enhancing its gas-sensing performance. Conversely, the addition of 5.0 mol% of cobalt led to an increase in particle size, which might have hindered sensor performance. Electrical characterization revealed that the $LaFeO_3$-Co sensor with 2.5 mol% doping achieved the highest response of 13.30 at 330°C and 270 ppm of acetone gas. This study underscores the promise of Co-doped $LaFeO_3$ in enhancing gas-sensing capabilities, marking a substantial advancement in the development of high-performance acetone gas sensors. However, further optimization and investigation are necessary to fully realize its potential for commercialization.

1. Introduction

Acetone gas (C_3H_6O) has an advantage in several sectors, such as industries and medicine, and is mainly used as a biomarker for the respiratory diagnosis of diabetes [1]. However, acetone is also known as a toxic, flammable, and harmful gas. Apart from that, long-term exposure to acetone can cause damage to the eyes and nose [2]. Moreover, it was reported that exposure of acetone in humans to more than 173 parts per million (ppm) could cause fatigue, excessive headaches, and nervous system damage [3]. Hence, the World Health Organisation (WHO) has declared that an acetone concentration exceeding 180 ppm indicates an unhealthy environment for individuals [4]. In light of the potential consequences resulting from acetone exposure, it is imperative to develop a gas sensor capable of detecting even trace amounts of acetone gas measured in ppm. This is done as a preventive measure against potential negative events.

Several researchers have focused on developing a gas sensor specifically for detecting acetone using metal oxide semiconductors (MOS). For now, MOS is the best material to apply as a gas sensor because it is small, low-cost, and easy to maintain [5]. Besides that, MOS has other advantages, i.e., high specific surface area and exposed crystal plane. These two things are the key factors showing the MOS's ability to detect gas [6]. Zinc oxide (ZnO), tin oxide (SnO_2), iron(III) oxide (Fe_2O_3), tungsten trioxide (WO_3), and lanthanum iron oxide (LaFeO) are commonly employed as primary materials for acetone gas sensors [7-11]. $LaFeO_3$ is currently a highly favoured material among researchers due to its excellent chemical stability [12]. Despite its potential for gas sensing applications, $LaFeO_3$ is limited by its relatively large particle size [13]. According to a study conducted by Islam *et al.* (2019), the addition of a dopant can be used to decrease the size of the particles [14].

According to the stated explanation, we presented the synthesis of $LaFeO_3$ with Co-doping, which was prepared using the co-precipitation method and transformed into a thick film using the screen-printing technique. Subsequently, it was utilized as a gas sensor for acetone. In addition, Co-doped materials were chosen for their favourable characteristics in promoting the deformation of a stable doping structure [15]. Moreover, the incorporation of a Co-dopant in $LaFeO_3$ enhances its ability to detect acetone. Jing *et al.* (2022) demonstrated that the resistance of $LaFeO_3$ was enhanced through Co-doping, resulting in improved gas sensor performance [16].

The doping of Co^{3+} into $LaFeO_3$ exhibits significant promise for research purposes. The concentration of Co-doped plays a crucial role in enhancing the performance of the gas sensor. In 2017, Li *et al.*

conducted a study that examined the use of 3 mol% of Co-doped material and observed a positive response [17]. This discovery prompts further investigation into the effects of Co-doping on $LaFeO_3$, specifically at concentrations of 2.5 mol% and 5.0 mol%. This study employed a margin of more than 3 mol% in the upper and lower ranges to examine the properties of $LaFeO_3$ in detecting acetone gas, which is affected by Co-doping. If this study identifies favourable attributes of a gas sensor, $LaFeO_3$ with Co-doping could be marketed as an acetone gas sensor to assist various industries in mitigating the harm caused by acetone.

2. Experimental detail

2.1 Chemicals

This work utilized the following chemicals: lanthanum(III) oxide (La_2O_3), iron(III) oxide (Fe_2O_3), cobalt(II) oxide (CoO), hydrochloric acid (HCl) 2.0 M, ammonium hydroxide (NH_4OH) 25%, and distilled water. The chemicals were utilized for synthesizing $LaFeO_3$ with co-doping without undergoing the purification process. Subsequently, the materials were transformed into a dense film by utilizing an alumina substrate, silver (Ag) paste, and organic vehicles comprising ethyl cellulose and α-terpineol. In this study, acetone with a concentration of 97% was utilized for experimental purposes.

2.2 Preparation of $LaFeO_3$ with co-doped

In this work, $LaFeO_3$ with co-doped was synthesized using the co-precipitation method as follow the previous work [18], as illustrated in Figure 1. The synthesis processes were conducted simultaneously three (3) times under identical conditions but with varying concentrations of co-doped, as indicated in Table 1. In the initial stage, the chemicals comprising La_2O_3, Fe_2O_3, and CoO are dissolved individually in 20 mL of HCl 0.2 M solution with the assistance of a magnetic stirrer for approximately 2 h. The solutions are then combined and agitated using a magnetic stirrer for approximately one hour to achieve a uniform mixture. Subsequently, a 25% NH_4OH solution is gradually introduced until the solution achieves a pH value of 7. Then, the solution is allowed to stand undisturbed for a duration of 24 h, resulting in the formation of the precipitate. The precipitate is filtered and rinsed three times with distilled water to remove impurities. The final step involves drying the precipitate at 100°C for 6 h, followed by calcination at 600°C for 3 h. The resulting product is Co-doped $LaFeO_3$ in the form of a brown powder.

2.3 Thick film preparation and acetone gas characterizations

The thick film preparation and gas characterization are conducted in accordance with the step-by-step procedure previously outlined [18]. This step began with making a gel from an organic vehicle containing 10 wt% ethyl cellulose and 90 wt% terpineol. The compounds were gradually mixed gradually for approximately one hour using a hand spatula or by manual stirring. Once a gel was formed, it remained undisturbed for one hour. The previously prepared $LaFeO_3$ powder, which had been doped with cobalt, was mixed with a gel in a 7:3 ratio using manual stirring until a uniform mixture was achieved. Then, the thick film was prepared using the screen-printing method, with the detailed procedure illustrated in Figure 2. The aforementioned procedures were conducted on the alumina substrate with dimensions of 1.0 cm × 0.5 cm × 0.5 mm, as depicted in Figure 2. The screen-printing techniques were employed for their advantageous properties, including the ability to create a smooth and flat surface with a thick film, which can enhance the performance of gas sensors [19].

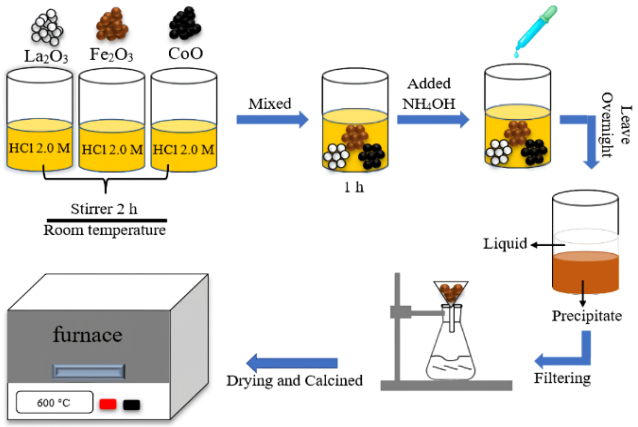

Figure 1. Illustration of the preparation of $LaFeO_3$ with Co-doped by co-precipitation method.

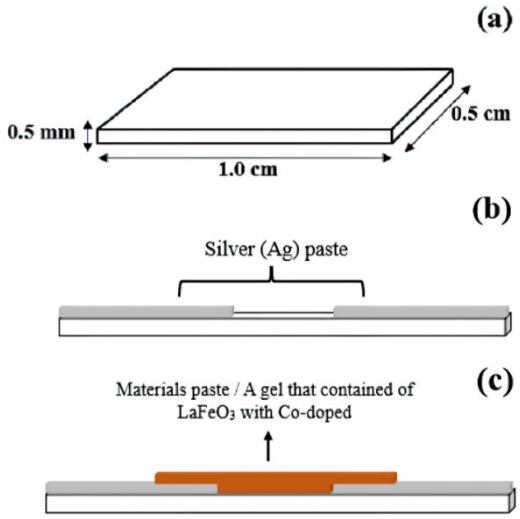

Figure 2. Thick film preparation (a) a size of alumina substrate, (b) silver (Ag) paste coating, (c) a gel of $LaFeO_3$ with Co-doped coating.

Table 1. The concentrations of Co-doped in $LaFeO_3$.

Samples	Composition [mol%]		
	La_2O_3	Fe_2O_3	CoO
$LaFeO_3$	50.0	50.0	0
$LaFeO_3$-Co-1	50.0	47.5	2.5
$LaFeO_3$-Co-2	50.0	45.0	5.0

Initially, the Ag paste was applied onto the alumina substrate as electrodes, following the pattern depicted in Figure 2(b), and then dried at a temperature of 600°C for 10 min. In the second step, a layer of Co-doped $LaFeO_3$ gel was applied onto the Ag silver as depicted in Figure 2(c), and then subjected it to a firing process at a temperature of 600°C for 2 h. Subsequently, the thick film is successfully produced once it meets the specified criteria, as depicted in Figure 3. It demonstrates the "OL" value in resistance measurements.

Furthermore, several characterizations were also carried out to verify the performance of thick film as acetone gas sensors, including crystal structure, morphological structure, and electrical properties. The crystal structure characterization was carried out using an X-ray diffractometer (XRD) with PANalytical X'Pert Pro Series PW3040/x0 to analyse the successful synthesis of $LaFeO_3$ with Co-doped. To determine the average crystallite size of $LaFeO_3$ with Co-doped, the Debye-Scherrer formula in Equation (1) was used [20-24]. These crystallite sizes were analysed for their effect on the performance of co-doped $LaFeO_3$ in binding acetone gas as the target [25].

Figure 3. Checking the feasibility process of the fabricated thick film.

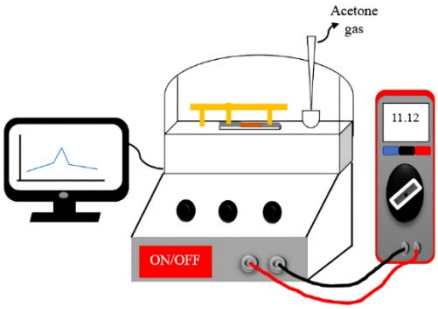

Figure 4. Illustration of electrical properties characterization processes.

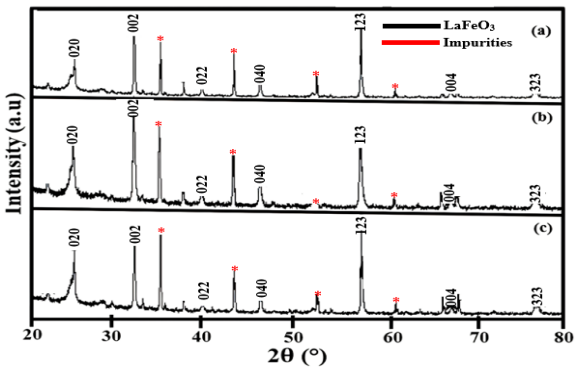

Figure 5. XRD pattern of (a) $LaFeO_3$; (b) $LaFeO_3$-Co-1; and (c) $LaFeO_3$-Co-2.

$$D = \frac{K\lambda}{B\cos\theta} \quad (1)$$

where D indicates the crystallite size (nm), K is the Scherrer number within the range of 0.9 to 1.0, respectively [26]. Sanjana states that the commonly used Scherrer number for analysing crystallite size is 0.9 [27]. In this study, a wavelength of 1.5406 Å was used for X-ray characterization. B represents the full width at half-maximum (FWHM), and θ represents the angle of Bragg's diffraction.

The morphological structure characterizations were analysed using the scanning electron microscopy (SEM) technique, specifically with the JEOL JSM-6360LA instrument. The purpose of this study was to analyse the properties of $LaFeO_3$ with Co-doped, focusing on the distribution of particles and the size of the grains. The variables were analysed for their impact on the performance of $LaFeO_3$ with Co-doped in binding acetone gas as the target [28]. Subsequently, analyses of electrical properties were performed to evaluate the effectiveness of Co-doped $LaFeO_3$ in binding acetone gas, particularly examining its responses to varying concentrations: 90 ppm, 180 ppm, and 270 ppm. This assessment utilized a gas chamber tool, as depicted in Figure 4. Characterization involved measuring the resistance of Co-doped $LaFeO_3$ in thick film form at 5 min intervals, incrementally raising the temperature from room temperature to 330°C. Additionally, the resistances are calculated using Equation (2) to determine the reactions of $LaFeO_3$ with co-doped when exposed to acetone gas [29-34].

$$\text{Response} = \frac{R_g}{R_a} \quad (2)$$

where R_g is the resistance value in the room containing acetone gas and R_a is the resistance value in the room with ambient conditions without acetone gas. The conditions were tested on a thick film based on $LaFeO_3$ with co-doping, respectively.

3. Results and discussions

The crystal structure of $LaFeO_3$ with co-doping is well-documented, as it plays a crucial role in the performance of acetone gas. The XRD pattern obtained from the characterization is analysed and depicted in Figure 5. The XRD peaks validate that the co-doped $LaFeO_3$ possesses cubic structures, as evidenced by the lattice parameters provided in Table 2. The comparison is based on the Crystallography Open Database (COD) number 96-154-2033 [35]. Furthermore, it has been verified that two distinct phases have been identified based on the XRD peaks, namely $LaFeO_3$ and aluminium oxide (Al_2O_3). The formation of the Al_2O_3 phase on the substrate is a result of insufficient thickness of the $LaFeO_3$ layer with co-doping that is applied to the substrate. Nevertheless, this is not a concern as there are no additional phases observed in the XRD patterns, suggesting the successful synthesis of co-doped $LaFeO_3$ without any impurities. Subsequently, the cobalt phase becomes undetectable in XRD peaks as a result of the complete replacement of Co^{3+} ions with Fe^{3+} ions in the $LaFeO_3$ lattice [36]. The occurrence can be attributed to the smaller ionic radius of Co^{3+} (61.0 Å) compared to Fe^{3+} (64.5 Å), which facilitates the substitution process [37].

From the analysis, it is known that the $LaFeO_3$ with co-doped were identified from the highest peaks of diffraction that appears at $2\theta = 32.35°$ (101), $2\theta = 32.12°$ (101), and $2\theta = 32.38°$ (101), respectively for $LaFeO_3$, $LaFeO_3$-Co-1, and $LaFeO_3$-Co-2 which matches to COD number of 96-154-2033. Then, the crystallite size is also calculated using Debye-Scherrer formula that is presented in Equation (1) with the results as shown in Table 2. Crystallite size plays a vital role in the gas sensor performances. According to Njoroge *et al.* (2022), the smaller crystallite size will increase the performances of gas sensors that consist of responses or sensitivity [38]. The smaller crystallite size will generate a high band gap of materials and cause electron transfer to occur with more barriers of electrons [39,40]. However, this phenomenon creates more active sites that are useful for the sensing processes and will increase the performances of gas sensors [41,42]. In this study, it was observed that there was a decrease in crystallite size after the addition of 2.5 mol% co-dopant. This decline in crystallite size can be attributed to the lattice distortion effect caused by the substitution of Co^{3+} ions, which possess a smaller ionic radius compared to Fe^{3+} as previously outlined. This distortion leads to the generation of internal stress within the $LaFeO_3$ lattice, thereby impeding the growth of crystallites and consequently resulting in reduced crystallite sizes. Conversely, at elevated dopant concentrations, specifically 5.0 mol% co-dopant, the crystallite size exhibits an increase. This phenomenon is attributed to the surplus of Co^{3+} ions, which induce agglomeration or grain growth due to their influence on lower surface energy. Consequently, this allows the crystallites to expand in size. Moreover, at elevated dopant concentrations, the distortion effect on the lattice is mitigated, thereby enabling the growth of crystallites. This condition relates to the morphological structural characterization conducted using SEM, which is informed by the smaller particle size, which also increases the performance of gas sensors [43]. The results are displayed as images with a specific magnification, as shown in Figure 6.

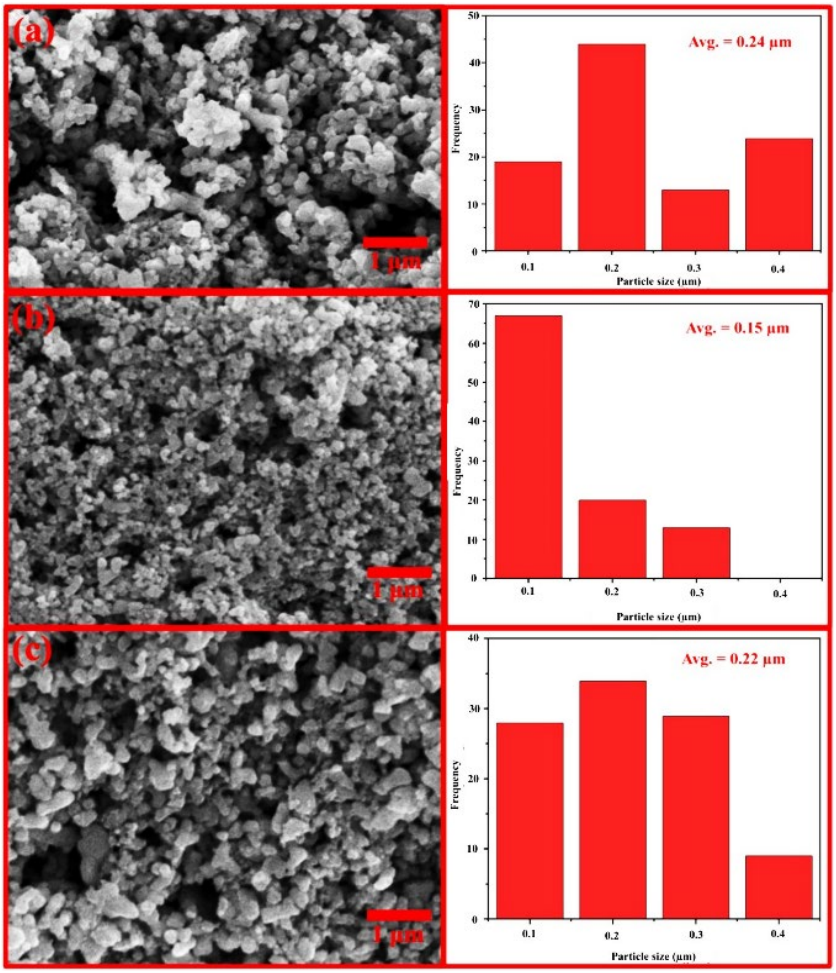

Figure 6. SEM image and particle size distribution of (a) $LaFeO_3$ (b) $LaFeO_3$-Co-1 (c) $LaFeO_3$-Co-2.

Table 2. Lattice parameters and crystallite size of $LaFeO_3$ with Co-doped.

Samples	Lattice parameters (a=b=c) [Å]	Crystallite size [nm]
$LaFeO_3$	3.9260	67.29
LaFeO3-Co-1	3.9208	43.53
LaFeO3-Co-2	3.9319	62.46

The analysis shows that the particle size of $LaFeO_3$ decreases when the co-doped has been added as much as 2.5 mol%. However, the particle size increased again when the co-doped addition exceeded 2.5 mol%, specifically reaching approximately 5.0 mol%. Thus, it is possible that $LaFeO_3$ with a 2.5 mol% concentration of co-doping exhibits superior gas sensing capabilities for detecting acetone gas.

Subsequently, an analysis was performed to characterise the electrical properties. The study revealed that $LaFeO_3$ with co-doping exhibits p-type gas sensor properties. The resistance measurements for different concentrations of acetone gas (specifically 90 ppm, 180 ppm, and 270 ppm) are depicted in Figure 7(a). A p-type gas sensor exhibits an increase in resistance when exposed to a specific target gas (in this case, acetone) [18,44]. This phenomenon can be attributed to the properties of p-type semiconductors, which possess holes as the predominant charge carriers due to the presence of cation vacancies in their crystal structure [45]. The interaction of acetone with adsorbed oxygen ions on the sensor's surface leads to the generation of electrons through chemical reactions, which subsequently combine with holes, thereby reducing the number of available holes. This decline in holes, in turn, results in a reduction in sensor conductivity, consequently increasing resistance [46]. As the target gas concentration increases, the number of electrons produced rises, leading to enhanced recombination with holes and subsequent increase in resistance [47]. Concurrently, at elevated temperatures, the resistance exhibits a tendency to decrease. This phenomenon can be attributed to the increased thermal energy, which facilitates the transition of electrons from the valence band to the conduction band, thereby creating additional holes in the valence band. The enhancement of hole concentration, in turn, promotes an increase in conductivity, consequently leading to a reduction in resistance. Additionally, the desorption of gas molecules from the semiconductor surface at elevated temperatures may also reduce the impact of the target gas on resistance [48]. The resistance was computed using Equation (2) and yielded the response value of $LaFeO_3$ with co-doped to the acetone gas, as depicted in Figure 7(b). At a concentration of 90 ppm, the sensor response exhibited an increase in comparison with the 180 ppm concentration. This finding suggests that, at low concentrations, acetone molecules are optimally adsorbed on the sensor surface, resulting in an even distribution of molecules that facilitates efficient interaction between the target gas and the active site of the sensor. This interaction leads to a reasonably high response. Conversely, at 180 ppm, the response diminished due to partial saturation or a blocking effect, where an excessive number of acetone molecules on the sensor surface restricts the access of new molecules to the active sites, leading to a reduced response. In contrast, at 270 ppm, the response exhibited a significant increase, reaching its maximum value. At this concentration, the maximum number of acetone molecules are adsorbed without causing excessive saturation, so the surface chemical reaction occurs optimally. The intensive interaction between the gas molecules and the sensor material results in a much higher response than the previous concentration is non-linear, influenced by adsorpsion conditions and surface reaction kinetics.

The highest response of $LaFeO_3$ with Co-doped is reached by $LaFeO_3$-Co-1 in 270 ppm, which is about 13.30 at the working temperature of 330°C. It means that the dopant also plays an important role in the gas sensor performance. According to Hu *et al.* (2017), the dopant increased the response of gas sensors due to their characteristics that help the main materials ($LaFeO_3$) on the binding of the O atom [49]. However, the addition of dopants in too high a concentration will decrease the gas sensor's performance due to their effect on reducing the active sites on the surface of materials ($LaFeO_3$). This condition will also reduce the surface interaction with the O atom, which has an effect on the decrease of sensor response [50]. This phenomenon was noticed on the gas sensors based on $LaFeO_3$-Co-2 due to their decreasing responses to the acetone gas compared to the $LaFeO_3$-Co-1. It might be possible that the co-dopant with a concentration of as much as 5.0 mol%, which is too high for $LaFeO_3$.The obtained outcome demonstrated a strong sensitivity of the gas sensor in detecting the specific gas target, namely acetone, in this study. The recognition of acetone as the target was achieved through the response of co-doped $LaFeO_3$, which reached 13.30 at a concentration of 270 ppm. This value is significantly higher than the previous study conducted on $LaFeO_3$ with various dopants under different reducing gases, as indicated in Table 3. Despite the elevated working temperature, further investigation is required to develop a gas sensor based on $LaFeO_3$ for this study.

The sensing mechanisms responsible for detecting acetone gas have been explained through the reaction of $LaFeO_3$ with Co-doping. These are gas sensors that function as p-type. $LaFeO_3$ exhibits a sensing mechanism that alters its resistance when exposed to air and acetone during the measurement processes. Wang (2019) proposed that this mechanism elucidates how the materials generate charge-carrier holes. Subsequently, the oxygen that the surface of the particle has absorbed undergoes ionization, transitioning from Oads- to O_2ads-, as a result of the capture of free electron particles [53]. The chemical reaction for the adsorption of oxygen is represented by Equations (3) to 6 below [54]:

$$O_2\ (gas) \rightarrow O_2\ (ads) \quad (3)$$

$$O_2\ (ads) + e^- \rightarrow O_2^-\ (ads)\ (T < 100\ °C) \quad (4)$$

$$O_2^-\ (ads) + e^- \rightarrow 2O^-\ (ads)\ (100\ °C < T < 300\ °C) \quad (5)$$

$$O^-\ (ads) + e^- \rightarrow O^{2-}\ (ads)\ (T > 300°C) \quad (6)$$

Furthermore, when the acetone is exposed to the sensor, the reaction will occur on the surface between the gas molecule and chemisorbed oxygen based on the reaction in Equation (7) to Equation (10) below [55]:

$$CH_3COCH_3\ (gas) \rightarrow CH_3COCH_3\ (ads) \quad (7)$$

$$CH_3COCH_3\ (ads) + O^-\ (ads) \rightarrow CH_3CO^+ + CH_3O^- + e^- \quad (8)$$

$$CH_3CO^+ \rightarrow CH_3+ + CO\ (ads) \quad (9)$$

$$CO\ (ads) + O\ (ads) \rightarrow CO_2 + e^- \quad (10)$$

Based on the explanation of sensing mechanisms, the acetone gas sensor based on $LaFeO_3$ with Co-doped that has been fabricated belongs to the gas sensor with a high working temperature. According to Mirzaei *et al.*, the reaction process of the gas sensor in detecting the acetone gas is limited by the diffusion rate of gas molecules [56]

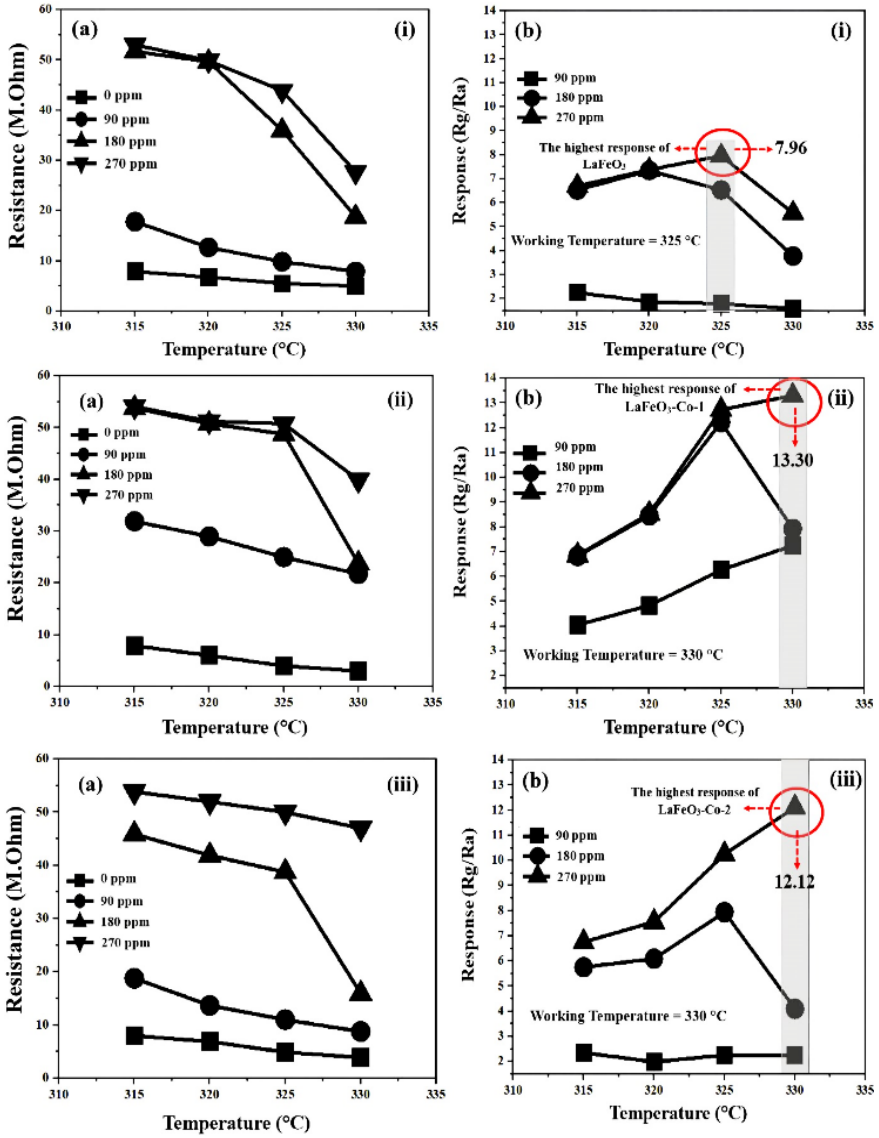

Figure 7. Electrical properties characterization (a) resistance of (i) $LaFeO_3$ (ii) $LaFeO_3$-Co-1 (iii) $LaFeO_3$-Co-2, (b) response to the acetone gas of (i) $LaFeO_3$ (ii) $LaFeO_3$-Co-1 (iii) $LaFeO_3$-Co-2.

Table 3. The comparison of $LaFeO_3$ response as gas sensors.

Samples	Gases	Response	Working Temperature [°C]	Ref.
$LaFeO_3$ with 2.5 mol% of Co-doped	Acetone	13.30	330	This work
$LaFeO_3/Fe_2O_3$ with 0.5 mol% of ZnO-doping	Ethanol	3.09	180	[18]
$LaFeO_3/Fe_2O_3$ with Ca-and-Co-doped	Ethanol	3.65	190	[51]
$LaFeO_3$ with SrO doping	Ethanol	3.05	300	[52]

4. Conclusions

In summary, $LaFeO_3$ with Co-doped has been successfully synthesized by the co-precipitation method and fabricated into a thick film using a screen-printing technique. The result shows that the co-doped plays an important role in improving the performance of $LaFeO_3$ gas sensors in detecting acetone gas. This work found that the addition of Co-dopant to $LaFeO_3$ at a concentration of about 2.5 mol% produced the highest response, which was 13.30 at the working temperature of 330°C and 270 ppm. However, the excess dopant reduced the gas sensor performance, as evidenced by the decreased response to 12.20 when 5.0 mol% of Co-dopant was added. Based on these findings, further study of dopant is required for the development of gas sensors based on semiconductors, especially the addition of co-dopant on $LaFeO_3$. Therefore, these conditions indicate that the commercializing acetone gas sensors based on Co-doped $LaFeO_3$ still requires more investigation to achieve better performances in the future.

Acknowledgements

This work was financially supported by Penelitian Pengembangan Kelompok Bidang Keilmuan (PPKBK) Universitas Pendidikan Indonesia Research Grants in the 2024 fiscal year.

References

[1] Q. Wang, X. Cheng, Y. Wang, Y. Yang, Q. Su, J. Li, B. An, Y. Luo, Z. Wu, and E. Xie, "Sea urchins-like WO_3 as a material for resistive acetone gas sensors," *Sensors and Actuators B: Chemical*, vol. 355, p. 131262, 2022.

[2] C. Li, P. G. Choi, K. Kim, and Y. Masuda, "High performance acetone gas sensor based on ultrathin porous NiO nanosheet," *Sensors and Actuators: B. Chemical*, vol. 367, p. 132143, 2022.

[3] L. Guo, Z. Shen, C. Ma, C. Ma, J. Wang, and T. Yuan, "Gas sensor based on MOFs-derived Au-loaded SnO_2 nanosheets for enhanced acetone detection," *Journal of Alloys and Compounds*, vol. 906, p. 164375, 2022.

[4] G. Feng, Y. Che, S. Wang, S. Wang, J. Hu, J. Xiao, C. Song, and L. Jiang, "Sensitivity enhancement of In_2O_3/ZrO_2 composite based acetone gas sensor: A promising collaborative approach of ZrO_2 as the heterojunction and dopant for in-situ grown octahedron-like particles," *Sensors and Actuators: B. Chemical,* vol. 367, p. 132087, 2022.

[5] C. Zhang, G. Liu, X. Geng, K. Wu, and M. Debliquy, "Metal oxide semiconductors with highly concentrated oxygen vacancies for gas sensing materials: A review," *Sensors and Actuators A: Physical*, vol. 309, p. 112026, 2020.

[6] T. Li, W. Yin, S. Gao, Y. Sun, P. Xu, S. Wu, H. Kong, G. Yang, and G. Wei, "The combination of two-dimensional nanomaterials with metal oxide nanoparticles for gas sensors: A review," *Nanomaterials*, vol. 12, p. 982, 2022.

[7] E. Wongrat, N. Chanlek, C. Cheaiarrom, W. Thupthimchun, B. Samransuksamer, and S. Choopun, "Acetone gas sensors based on ZnO nanostructures decorated with Pt and Nb," *Ceramics International*, vol. 43, pp. S557-S566, 2017.

[8] X. Lian, Y. Li, X. Tong, Y. Zou, X. Liu, D. An, and Q. Wang, "Synthesis of Ce-doped SnO_2 nanoparticles and their acetone gas sensing properties," *Applied Surface Science*, vol. 407, pp. 447-455, 2017.

[9] S. Liang, J. Li, F. Wang, J. Qin, X. Lai, and X. Jiang, "Highly sensitive acetone gas sensor based on ultrafine α $-Fe_2O_3$ nano-particles," *Sensors and Actuators B: Chemical*, vol. 238, pp. 923-927, 2017.

[10] J. Zhang, H. Lu, C. Yan, Z. Yang, G. Zhu, J. Gao, F. Yin, and C. Wang, "Fabrication of conductive graphene oxide WO_3 composite nanofibers by electrospinning and their enhanced acetone gas sensing properties," *Sensors and Actuators B: Chemical*, vol. 264, pp. 128-138, 2018.

[11] H. Zhang, H. Qin, C. Gao, G. Zhou, Y. Chen, and J. Hu, "UV light illumination can improve the sensing properties of $LaFeO_3$ to acetone vapor," *Sensors*, vol. 18, p. 1990, 2018.

[12] I. Jaouali, H. Hamrouni, N. Moussa, M. F. Nsib, M. A. Centeno, A. Bonavita, G. Neri, and S. G. Leonardi, "$LaFeO_3$ ceramics as selective oxygen sensors at mild temperature," *Ceramics International*, vol. 44, pp. 4183-4189, 2018.

[13] N. Sivakumar, J. Gajendiran, A. Alsalme, and K. Tashiro, "Structural, morphological, optical, magnetic and electrochemical behaviour of solid state synthesized pure and Sr-doped $LaFeO_3$ nanoparticles," *Physica B: Condensed Matter*, vol. 641, pp. 414086, 2022.

[14] M. R. Islam, M. Rahman, S. F. U. Farhad, and J. Podder, "Structural, optical and photocatalysis properties of sol-gel deposited Al-doped ZnO thin films," *Surfaces and Interfaces*, vol. 16, pp. 120-126, 2019.

[15] Y. Chen, J. Wu, Z. Xu, W. Shen, Y. Wu, and J. Corriou, "Computational assisted tuning of Co-doped TiO_2 nanoparticles for ammonia detection at room temperatures," *Applied Surface Science*, vol. 601, p. 154214, 2022.

[16] Z. Jing, Z. Zhong, C. Zhang, and Q. Gao, "Co-doped $LaFeO_3$ gas sensor for fast low-power acetone detection," *Journal of Nanoelectronics and Optoelectronics*, vol. 17, pp. 775-784, 2022.

[17] Z. Li, A. A. Haidry, B. Gao, T. Wang, and Z. Yao, "The effect of Co-doping on the humidity sensing properties of ordered mesoporous TiO_2," *Applied Surface Science*, vol. 412, pp. 638-647, 2017.

[18] E. Suhendi, A. E. Putri, M. T. Ulhakim, A. Setiawan, and D. G. Syarif, "Investigation of ZnO doping on $LaFeO_3/Fe_2O_3$ prepared from yarosite mineral extraction for ethanol gas sensor application," *AIMS Materials Science*, vol. 9, pp. 105-118, 2022.

[19] X. Peng, J. Liu, Y. Tan, R. Mo, and Y. Zhang, "A CuO thin film type sensor via inkjet printing technology with high reproducibility for ppb-level formaldehyde detection," *Sensors and Actuators: B. Chemical*, vol. 362, p. 131775, 2022.

[20] L. Lv, P. Cheng, Y. Zhang, Y. Zhang, Z. Lei, Y. Wang, L. Xu, Z. Weng, and C. Li, "Ultra-high response acetone gas sensor based on $ZnFe_2O_4$ pleated hollow microspheres prepared by green NaCl template," *Sensors and Actuators: B. Chemical*, vol. 358, p. 131490, 2022.

[21] L. Lv, Y. Wang, P. Cheng, Y. Zhang, Y. Zhang, Z. Lei, L. Xu and Z. Wei, "Production of MFe_2O_4 (M = Zn, Ni, Cu, Co and Mn) multiple cavities microspheres with salt template to assemble a high-performance acetone gas sensor," *Journal of Alloys and Compounds*, vol. 904, p. 164054, 2022.

[22] B. H. Waghchaure, V. A. Adole, B. S. Jagdale, and P. B. Koli, "Fe^{3+} modified zinc oxide nanomaterial as an efficient, multifaceted material for photocatalytic degradation of MB dye and ethanol gas sensor as part of environment rectification," *Inorganic Chemistry Communications*, vol. 140, p. 109450, 2022.

[23] S. Paneru, and D. Kumar, "Ag-doped-CuO nanoparticles supported polyaniline (PANI) based novel electrochemical sensor for sensitive detection of paraoxon-ethyl in three real samples," *Sensors and Actuators: B. Chemical,* vol. 379, p. 133270, 2023.

[24] K. Suganthi, E. Vinoth, L. Sudha, P. Bharathi, and M. Navaneethan, "Manganese (Mn^{2+}) doped hexagonal prismatic zinc oxide (ZnO) nanostructures for chemiresistive NO_2 sensor," *Sensors and Actuators: B. Chemical*, vol. 380, p. 133293, 2023.

[25] C. Rana, S. R. Bera, and S. Saha, "growth of SnS nanoparticles and its ability as ethanol gas sensor," *Journal of Materials Science: Materials in Electronics*, vol. 30, pp. 2016-2029, 2019.

[26] B. A. Krishna, P. N. Kumar, and P. Prema, "Green synthesis of copper oxide nanoparticles using Cinnamomum malabatrum leaf extract and its antibacterial activity," *Indian Journal of Chemical Technology (IJCT)*, vol. 27, pp. 525-530, 2020.

[27] D. V. S. Sanjana, B. Balraj, C. Siva, and S. Amuthameena, "Green hydrothermal synthesis of Ga doping derived 3D ZnO nanosatellites for high sensitive gas sensors," *Sensors and Actuators: B. Chemical,* vol. 379, p. 133215, 2023.

[28] G. Manjunath, S. Pujari, D. R. Patil, and S. Mandal, "A scalable screen-printed high performance ZnO-UV and gas sensor: effect of solution combustion," *Materials Science in Semiconductor Processing*, vol. 107, p. 104828, 2020.

[29] M. T. Rahman, M. S. A. Bhuiyan, M. J. Islam, K. M. Reza, A. Gurung, and Q. Qiao, "A flexible, ultrasensitive, and highly selective bi-functional acetone and ethanol gas sensor," *2022 12th International Conference on Electrical and Computer Engineering (ICECE)*, Dhaka, Bangladesh, pp. 84-87, 2022.

[30] J. Walker, P. Karnati, S. A. Akbar, and P. A. Morris, "Selectivity mechanisms in resistive-type metal oxide heterostructural gas sensors," *Sensors and Actuators: B. Chemical*, vol. 355, p. 131242, 2022.

[31] H. Y. Lee, J. H. Bang, S. M. Majhi, A. Mirzaei, K. Y. Shin, D. J. Yu, W. Oum, S. Kang, M. L. Lee, S. S. Kim, and H. W. Kim, "Conductometric ppb-level acetone gas sensor based on one-pot synthesized Au @Co_3O_4 core-shell nanoparticles," *Sensors and Actuators: B. Chemical,* vol. 359, p. 131550, 2022.

[32] Q. Yu, X. Gong, Y. Jiang, L. Zhao, T. Wang, F. Liu, X. Yang, X. Liang, F. Liu, P. Sun, and G. Lu, "Bimetallic MOFs-derived core-shell structured mesoporous Sn-doped NiO for conductometric ppb-level xylene gas sensors," *Sensors and Actuators: B. Chemical*, vol. 372, p. 132620, 2022.

[33] B. Song, M. Yang, L. Liu, X. Zhang, Z. Deng, Y. Xu, L. Huo, and S. Gao, "Biotemplate-derived mesoporous Cr_2O_3 tube bundles for highly sensitive and selective detection of trace acetone at low temperature," *Chemical Engineering Journal*, vol. 450, p. 138211, 2022.

[34] S. Li, C. Wang, Z. Lei, S. Sun, J. Gao, P. Cheng, and H. Wang, "Synergistic adsorption effect on Co_3O_4(110) surface to promote the ethanol sensing properties: Experiment and theory," *Applied Surface Science*, vol. 612, p. 155776, 2023.

[35] H. Haryadi, D. G. Syarif, and E. Suhendi, "The effect of couple doping Gd and Co on the physical characteristics of $LaFeO_3$ thick film for acetone gas sensor application," *Jurnal Penelitian Fisika dan Aplikasinya (JPFA)*, vol. 12, pp. 115-126, 2022.

[36] C. Cao, J. Li, Y. Hu, L. Zhang, and W. Yang, "Mechanism investigation of A-site doping on modulating electronic band structure and photocatalytic performance towards CO_2 reduction of $LaFeO_3$ perovskite," *Nano Research*, vol. 17, pp. 3733-3744, 2024.

[37] H. Zhang, R. Zhang, Z. wu, F. Yang, M. Luo, G. Yao, Z. Ao, and B. Lai, "Cobalt-doped boosted the peroxymonosulfate activation performance of $LaFeO_3$ perovskite for atrazine degradation," *Chemical Engineering Journal*, vol. 452, p. 139427, 2023.

[38] M. A. Njoroge, N. M. Kirimi, and K. P. Kuria, "Spinel ferrites gas sensors: a review of sensing parameters, mechanism and the effects of ion substitution," *Critical Review in Solid State and Materials Sciences*, vol. 47, pp. 807-836, 2022.

[39] K. Chen, Y. Zhou, R. Jin, T. Wang, F. Liu, C. Wang, X. Yan, P. Sun, and G. Lu, "Gas sensor based on cobalt-doped 3D inverse opal SnO_2 for air quality monitoring," *Sensors and Actuators: B. Chemical*, vol. 350, p. 130807, 2022.

[40] N. M. Yusof, S. Ibrahim, and S. Rozali, "Advances on graphene-based gas sensors for acetone detection based on its physical and chemical attributes," *Journal of Materials Research*, vol. 37, pp. 405-423, 2022.

[41] B. Zhou, S. Yang, X. Jiang, and W. Song, "Experimental study on oxygen adsorption capacity and oxidation characteristics of coal samples with different particle sizes," *Fuel*, vol. 331, p. 125954, 2023.

[42] X. Bai, Z. Liu, H. Lv, J. Chen, M. Khan, J. Wang, B. Sun, Y. Zhang, K. Kan, and K. Shi, "N-doped three-dimensional needle-like CoS_2 bridge connection Co_3O_4 core-shell structure as high-efficiency room temperature NO_2 gas sensor," *Journal of Hazardous Materials*, vol. 423, p. 127120, 2022.

[43] H. Fu, Z. Feng, S. Liu, P. Wang, C. Zhao, and C. Wang, "Enhanced ethanol sensing performance of N-doped ZnO derived from ZIF-8," *Chinese Chemical Letters*, vol. 34, p. 107425, 2023.

[44] P. Srinivasan, M. Ezhilan, A. J. Kulandaisamy, K. J. Babu, and J. B. B. Rayappan, "Room temperature chemiresistive gas sensors: challenges and strategies – a mini review," *Journal of Materials Science: Materials in Electronics*, vol. 30, pp. 15825-15847, 2019.

[45] J. H. Choi, J. S. Seo, H. E. Jeong, K. Song, H. Baek, S. E. Shin, and Y. Qian, "Effect of field-effect and schottky heterostcructure on p-type graphene-based gas sensor modified by n-type In_2O_3 and phenylenediamine," *Applied Surface Science*, vol. 578, p. 152025, 2022.

[46] W. Qin, Z. Yuan, Y. Shen, R. Zhang, and F. Meng, "Phosphorus-doped porous perovskite $LaFe_{1-x}P_xO_{3-\delta}$ nanosheets with rich surface oxygen vacancies for ppb level acetone sensing at low temperature," *Chemical Engineering Journal*, vol. 431, p. 134280, 2022.

[47] S. Shah, S. Hussain, L. A. Khan, K. Yusuf, R. K. Manavalan, Y. Tianyan, X. Zhang, G. Liu, and G. Qiao, "ppb-level H_2 gas-sensor based on porous Ni-MOF derived NiO@CuO nanoflowers for superior sensing performance," *Materials Research Bulletin*, vol. 180, p. 11321, 2024.

[48] B. Yang, N. V. Myung, and T. Tran, "1D metal oxide semi-conductor materials for chemiresistive gas sensors: a review," *Advanced Electronic Materials*, vol. 7, p. 2100271, 2021.

[49] X. Hu, Z. Zhu, C. Chen, T. Wen, X. Zhao, and L. Xie, "Highly sensitive H_2S gas sensors based on Pd-doped CuO nanoflowers with low operating temperature," *Sensors and Actuators B: Chemical*, vol. 253, pp. 809-817, 2017.

[50] N. Sun, Q. Tian, W. Bian, X. Wang, H. Dou, C. Li, Y. Zhang, C. Gong, X. You, X. Du, P. Yin, X. Zhao, Y. Yang, X. Liu,

Q. Jing, and B. Liu, "Highly sensitive and lower detection-limit NO_2 gas sensor based on Rh-doped ZnO nanofibers prepared by electrospinning," *Applied Surface Science*, vol. 614, pp. 156213(1-10), 2023.

[51] E. Suhendi, Z. L. Amanda, M. T. Ulhakim, A. Setiawan, and D. G. Syarif, "The enhancement of ethanol gas sensors response based on calcium and zinc co-doped $LaFeO_3/Fe_2O_3$ thick film ceramics utilizing yarosite minerals extraction as Fe_2O_3 precursor," *Journal of Metals, Materials and Minerals*, vol. 31, pp. 71-77, 2021.

[52] E. Suhendi, M. T. Ulhakim, A. Setiawan, and D. G. Syarif, "The effect of SrO doping on $LaFeO_3$ using yarosite extraction based ethanol gas sensors performance fabricated by co-precipitation method," *International Journal of Nanoelectronics and Materials*, vol. 12, pp. 185-192, 2019.

[53] C. Wang, Q. Rong, Y. Zhang, J. Hu, B. Zi, Z. Zhu, J. Zhang, and Q. Liu, "Molecular imprinting Ag-$LaFeO_3$ spheres for highly sensitive acetone gas detection," *Materials Research Bulletin*, vol. 109, pp. 265-272, 2019.

[54] K. Yang, J. Ma, X. Qiao, Y. Cui, L. Jia, and H. Wang, "Hierarchical porous $LaFeO_3$ nanostructure for efficient trace detection of formaldehyde," *Sensors and Actuators B: Chemical*, vol. 313, p. 128022, 2020.

[55] H. Wu, F. Meng, X. Gong, W. Tao, L. Zhao, T. Wang, F. Liu, X. Yan, P. Sun, and G. Lu, "A solution to boost acetone sensing performance of perovskite oxides chemiresistors: In-situ derived p-p heterostructures," *Sensors and Actuators: B. Chemical*, vol. 378, p. 133092, 2023.

[56] A. Mirzaei, J. Lee, S. M. Majhi, M. Weber, M. Bechelany, H. W. Kim, and S. S. Kim, "Resistive gas sensors based on metal-oxide nanowires," *Journal of Applied Physics*, vol. 126, p. 241102, 2019.